Songklanakarin J. Sci. Technol.
31 (5), 517-525, Sep. - Oct. 2009

Songklanakarin Journal of Science and Technology
http://www.sjst.psu.ac.th

Original Article

Evaluation of bactericidal activity of TiO_2 photocatalysts: a comparative study of laboratory-made and commercial TiO_2 samples

Uraiwan Sirimahachai[1], Souwalak Phongpaichit[2] and Sumpun Wongnawa[1]*

[1] *Department of Chemistry,*

[2] *Department of Microbiology, Faculty of Science,*
Prince of Songkla University, Hat Yai, Songkhla, 90112 Thailand.

Received 17 February 2009; Accepted 25 May 2009

Abstract

Titanium dioxide photocatalysts were synthesized by sol-gel process, by varying the reaction conditions, acids, water content, and trivalent (Al, B) dopants. The characterizations of products were determined by XRD, SEM, BET, and UV-vis spectroscopy. The samples were mainly amorphous with a small amount of anatase, rutile, or a mixture of anatase and rutile, with a crystallite sizes of about 5-10 nm. The antibacterial activity of the synthesized TiO_2 samples were investigated qualitatively and semi-quantitatively. Five types of bacteria, *Escherichia coli* ATCC25922, *Psudomonas aeruginosa* ATCC27853, *Bacillus subtilis* BGA, *Staphylococcus aureus* ATCC25923, and *methicillin-resistant S. aureus* (MRSA) DMST 2054, were used for the inactivation experiment employing the agar dilution method. All the synthesized samples showed inactivation activity with varying degree of efficiency. Two of them showed a much higher activity than Degussa P25.

Keywords: titanium dioxide photocatalyst, antibacterial activity, photocatalytic process, sol-gel method, amorphous titanium dioxide

1. Introduction

Photocatalytic processes are rapidly developing as potential techniques for the purification of water and air (Legrini *et al.*, 1993; Mills and Hunte, 1997; Jacoby *et al.*, 1998; Lin and Li 2003). Among various metal oxide semiconductor photocatalysts, titanium dioxide is a very important photocatalyst due to its strong oxidizing power, nontoxicity, and photostability. The titania photocatalytic performance has been known to be dependent on several variables, such as, preparation method, particle size, reactive surface area, and ratio between anatase and rutile phases (Hoffmann *et al.*, 1995). Attempts have been made to improve the activity of titania photocatalyst through modified synthesis methods in order to alter the morphology and crystallinity, while dopings with ions of other elements are also another promising method.

Titania has three different crystalline phases: rutile, anatase, and brookite. Rutile is thermodynamically stable, while the latter two phases are in metastable states (Gopal *et al.*, 1997). Titania in anatase crystalline form behaves as a classical semiconductor. When a TiO_2 photocatalyst was illuminated by photons with energy greater than its band gap, an electron can be excited to the conduction band thus creating an electron-hole pair. With holes (h^+) and hydroxyl radicals ($OH^\bullet$) generated in the valence band, and electrons and superoxide anions ($O_2^{\bullet-}$) generated in the conduction band, irradiated TiO_2 photocatalysts can decompose and mineralize organic compounds by a series of oxidation reactions leading to carbon dioxide. It is also documented that inactivation of bacteria is caused by exposure to reactive oxygen intermediates, such as hydroxyl radicals ($OH^\bullet$), superoxide anion ($O_2^{\bullet-}$), and hydrogen peroxide (H_2O_2), which can damage proteins, nucleic acids, and cell membranes

*Corresponding author.
Email address: sumpun.w@psu.ac.th

(Ireland *et al.*, 1993; Ibanez *et al.*, 2003). In addition to water and wastewater disinfection, the semiconductor photocatalysis has received considerable attention over the past few years with emphasis given on the inactivation of bacteria, viruses, and protozoan parasites (Otaki *et al.*, 2000; Cho *et al.*, 2004; Rincon and Pulgarin 2004; Fernandez *et al.*, 2005; Lonnen *et al.*, 2005; Gumy *et al.*, 2006; Rincon and Pulgarin 2006). In terms of antibacterial effects of photocatalysts, Matsunaga *et al.* first reported the sterilization of microbial cells in water by a TiO_2/Pt powder in 1985. Since then, much research has been performed on the antibacterial effects of TiO_2 thin film, as well as TiO_2 powder (Huang *et al.*, 2000; Rincon and Pulgarin 2003; Yao *et al.*, 2007).

Until today, most of the work involving the disinfection of microorganisms by TiO_2 utilized commercial products, such as Degussa P25, anatase, rutile (Maness *et al.*, 1999; Rincon and Pulgarin 2003; Dadjour *et al.*, 2006; Benabbou *et al.*, 2007; Pal *et al.*, 2007; Sichel *et al.*, 2007; Sökmen *et al.*, 2007). In our laboratory, several modifications of titania nanoparticle have been synthesized for the dye degradation purpose, such as the acid catalysed nanosized TiO_2, Al(III)- and B(III)-doped TiO_2. Some data on the characterizations and physical properties of these synthesized TiO_2 powders have been reported elsewhere (Kanna and Wongnawa, 2008). In order to extend the usefulness of these photocatalysts, the antibacterial activities have been investigated in comparison with the commercial products and are reported in this article.

2. Materials and Methods

2.1 Materials

The main chemicals are titanium tetrachloride ($TiCl_4$, Merck, Germany), Degussa P25 (Degussa AG, Frankfurt, Germany), anatase (Carlo Erba, Italy), and rutile (R706, Dupont, USA). All other reagents were of reagent grade and used without further purification. Deionized water was used throughout the experiment. All solutions and materials in testing disinfection of TiO_2 were sterilized by autoclaving. The bacteria, *E. coli* ATCC25922, *P. aeruginosa* ATCC 27853, *B. subtilis* BGA, *S. aureus* ATCC25923 and MRSA SK1 were obtained from the laboratory stock of the Department of Microbiology, Faculty of Science, Prince of Songkla University.

2.2 Preparation of acid catalyzed nanosized TiO_2

Nanosized TiO_2 was synthesized from titanium tetrachloride. 20 mL of $TiCl_4$ was added slowly to 200 mL of cold deionized water (2°C), which had been placed in an ice-water bath at least 10 minutes prior to the addition. The solution was then mixed with 2 mL of conc. acid (HCl and H_2SO_4) and refluxed at 80°C for 1 h under vigorous stirring. The solution was then treated with ammonia solution until pH ≈ 7 and maintained at the same temperature for 24 hrs. The white precipitate formed was filtered and then washed with deionized water until no chloride ion was found by $AgNO_3$ solution test. The product was dried overnight at 105°C and ground to fine powder, until a final white powder was obtained. These samples are designated as TiO_2-200w-80HCl and TiO_2-200w-80H_2SO_4 (Kanna and Wongnawa, 2008).

2.3 Preparation of Al(III)- and B(III)-doped TiO_2

$TiCl_4$ was slowly added to deionized water ($TiCl_4$:H_2O volume ratios was 1:7.5 and 1:2.5) at room temperature. For the Al(III)-doped titania, $Al_2(SO_4)_3.18H_2O$ (0.04 mol% Al) and 2 mL of conc. HCl were added into the solution; then the mixture was kept over night without stirring. After that the resulting clear solution was refluxed at 95°C for 13 hrs. The solution was treated with ammonia solution to adjust the pH to 7 and continually refluxed for 13 hrs. This treatment produced a milky white TiO_2 suspensions. Afterwards the suspension was filtered, washed, and dried to obtain the final product as white powder. In the case of B (III)-doped titania, B_2O_3 (0.08 mol% B) was used instead of $Al_2(SO_4)_3.18H_2O$.These samples are designated as: TiO_2-Al150w, TiO_2-Al50w, TiO_2-B150w, and TiO_2-B50w (Suwanchawalit, 2005). The suffixes 150w and 50w correspond to high and low volume of water used.

2.4 Products characterization

Powder X-ray diffraction (XRD, PHILIPS X' Pert MPD with Ni-filtered and Cu Ka radiation**)** was used for crystal phase identification. The crystallite size has been calculated by using the Scherrer's formula,

$$L = \frac{K\lambda}{\beta_{hkl}\cos\theta} \quad (1)$$

where L is the average crystallite size in nm, K is a constant usually taken as 0.9, λ is the wavelength of the X-ray radiation (using CuK_α = 0.154056 nm), β_{hkl} is the line width at half-maximum height in radians, and θ is the diffracting angle (Zielinska *et al.*, 2001; Sivalingam *et al.*, 2003).

The Brunauer-Emmett-Teller (BET) surface area of TiO_2 powders were determined using Coulter, model SA 3100. The infrared spectra were investigated by a Bruker EQUINOX 55, in the range 4000-400 cm^{-1}. Scanning electron microscopy (SEM) images were obtained using a JEOL JSM-5800LV electron microscope.

The diffuse reflectance spectra of the solid catalysts were performed on a Shimadzu UV-2401PC spectrophotometer. $BaSO_4$ was used as reference and the spectra were recorded in the range of 200-600 nm. The bandgap energy (E_g) of the catalyst was calculated by the Planck's equation,

$$E_g = \frac{hc}{\lambda} = \frac{1240}{\lambda} \quad (2)$$

where E_g is the bandgap energy (eV), h is the Planck's constant, c is the light velocity ($3x10^8$ m/s), and λ is the

wavelength of the absorption edge (nm).

2.5 Culture of microorganisms

The bacteria, *E. coli* ATCC25922, *P. aeruginosa* ATCC27853, *B. subtilis* BGA, *S. aureus* ATCC25923, and MRSA DMST2054, were used for the antibacterial activity test for the photocatalyst. All bacteria were cultured overnight at 37°C in nutrient agar (NA). The density of final inocula contained 10^4 organisms/spot on the titanium dioxide. A bacterial inoculum was prepared by picking couple colonies of overnight growth culture into 1 mL nutrient broth and incubated them with agitation under aerobic condition at 35°C for 3 hrs. A 0.5 McFarland standard was used for visual comparison to adjust the suspension to a density equivalent to approximately 10^8 CFU/mL by using 0.85% saline solution. Then the suspensions of organisms was diluted in 0.85% saline solution to give 10^7 CFU/mL. Plates have been inoculated within 30 min to avoid any changes in the inoculum density.

2.6 Antibacterial activity test

Commercial anatase, rutile, Degussa P25, and the synthesized TiO_2 samples were used for all experiments. The method for testing the antibacterial activity is the agar dilution method to determine the minimal inhibitory concentration (MIC) of antimicrobial agents. The MIC is the lowest concentration of the agent that completely inhibits visible growth as judged by the naked eyes, disregarding a single colony or a thin haze within the area of the inoculated spot. The procedure, based on the recommendations from the Clinical and Laboratory Standard Institute (CLSI) for this method using a suspension of TiO_2 photocatalyst, was adapted to the agar dilution susceptibility test in this work (Approved standard M7-A4, 2002).

In each antibacterial test experiment, titanium dioxide agar plates were prepared in four concentrations 100, 50, 25, and 12.5 mg/ml in Mueller-Hinton agar (MHA). The weighed titanium dioxide powders were incorporated in 10 mL of melted MHA and poured into Petri dishes. The pH of each batch of medium was about 6.9. By using inoculum-replicating apparatus, the final inocula contained 10^4 CFU/spot, three spots/bacterial strain as shown in Figure 1. After inoculation, test plates were allowed to dry at room temperature before irradiation under UV light for a predetermined time was carried out.

The synthesized titanium dioxide agar plates were irradiated in an UV box, which contained five fluorescent blacklight tubes, 20 W each, with λ_{max} 366 nm (Randorn *et al.*, 2004). The sample plates were collected immediately after the titanium dioxide agar plates were exposed to UV light and subsequently every 30 min. The test plates were incubated at 35°C for 18 hrs. The results then were inspected visually and MIC values were recorded. All tests and inoculation on each plate were run in duplicate.

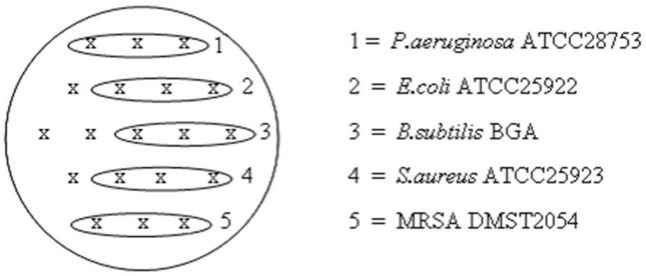

Figure 1. Titanium dioxide agar plate inoculated with various types of bacteria.

Figure 2. a) Agar plate with 25 mg/mL of TiO_2-200w-80H_2SO_4 irradiated under UV light for 30 min, b) control plate without TiO_2, and c) agar plate with 12.5 mg/mL of TiO_2-200w-80H_2SO_4 irradiated under UV light for 30 min.

A control plate was carried out under the same conditions with antibacterial activity test but without TiO_2 powders. Photographs of typical agar plates are shown in Figure 2.

3. Results and discussion

3.1 Physical properties of nanosized TiO_2 and Al(III)-, B(III)-doped TiO_2

The sol-gel method was used to synthesized the TiO_2 samples with two different acids, HCl and H_2SO_4, as catalysts in the hydrolysis process. The XRD results in Figure 3 show that varying the synthesis parameters affected the growth of anatase and rutile to some extent. When using H_2SO_4 or Al (III)-doped and prepared with a large amount of water the products were mainly amorphous TiO_2 with small amount of anatase phase. However, with HCl acid or Al(III)-doped and prepared with a small amount of water or B(III)-doped and prepared with a large amount of water mixtures of mainly amorphous titania with small amounts of both anatase and rutile phase were obtained. The presence of sulfate has been known to accelerate the growth of the TiO_2 cluster in the anatase phase. In this study, when H_2SO_4 was added as an acid catalyst in the hydrolysis process, the formation of anatase could be observed, since the SO_4^{2-} ion induced the growth of anatase phase (Zhang *et al.*, 1999; Zhang *et al.*, 2000; Kanna and Wongnawa, 2008).

The surface area of these synthesized samples are relatively high (Table 1, last column) due to its low crystallinity.

Table 1. Physical properties of commercial and synthesized TiO_2 samples.

Sample	Crystallinity [a] (%)	Crystallite size [b] (nm)		BET (m^2/g)
		Anatase	Rutile	
Anatase	100 (A)	13.4	-	11.3
Rutile	100 (R)	-	11.6	13.1
Degussa P25	80 (A), 20 (R) [c]	10.1	11.6	65.9
TiO_2-200w-80HCl	13 (A), 6 (R)	6.7	6.7	250.2
TiO_2-200w-80H_2SO_4	15 (A)	5.4	-	320.1
TiO_2-Al-150w	23.4 (A)	6.7	-	277.1
TiO_2-Al-50w	9.1 (A), 11.5 (R)	5.4	4.5	244.9
TiO_2-B-150w	6.3 (A), 6.8 (R)	6.7	10.1	234.8
TiO_2-B-50w	48.3 (R)	-	6.4	106.6

[a] Determined by XRD using standard addition method, the rest is amorphous phase. A denotes anatase and R denotes rutile. [b] Calculated from XRD data.
[c] Stylidi *et al.* (2004)

It is the aim of our project to study the samples right from the synthesis without calcinations (Kanna and Wongnawa, 2008). Therefore, without the calcination, the samples remain mostly in the amorphous form with a small amount of crystalline phases (anatase and rutile) as shown by the XRD patterns in Figure 3. The small amount of each anatase phase or rutile phase was determined by using XRD data combined with the standard addition method and shown in the second column of Table 1. The crystallite sizes of anatase and rutile (column 3 and 4 of Table 1) were calculated from the Sherrrer's formula (Equation 1). According to these sizes they can be classified as nanoparticles. The bandgap energies were obtained from the absorption edge wavelengths in Figure 4 and calculated by Equation 2. The corresponding numerical data are shown in Table 2. None of the bandgap energies show a significant deviation from the normal values of anatase and rutile.

The SEM images (Figure 5 and 6) show the morphology of the samples and appear to be constituted of spherical building units. The synthesized samples, which exist mostly in amorphous phase, show higher aggregation with the formation of bigger chunks than the commercial samples. This could be the result from the non- calcination at high temperature being applied.

3.2 Evaluation of antibacterial activity of TiO_2

The bactericidal acvitity of synthesized and commercial TiO_2 nanoparticles were evaluated by growth inhibition of *P. aeruginosa*, *E. coli* (the Gram-negative bacteria), and *B. subtilis*, *S. aureus*, MRSA (the Gram-positive bacteria). The Gram-positive bacteria have a relatively thick wall composed of many layers of peptidoglycan polymer and only one layer of membrane. The Gram-negative bacteria have only a thin layer of peptidoglycan and a more complex cell wall with two cell membranes, an outer membrane, and a plasma

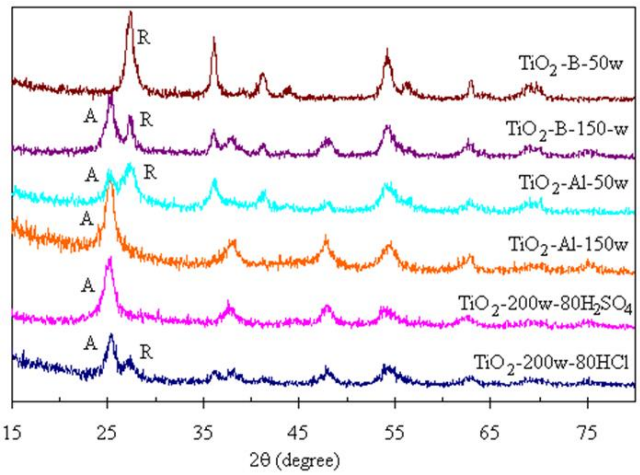

Figure 3. XRD patterns of all the synthesized TiO_2 samples; A denotes anatase and R denotes rutile.

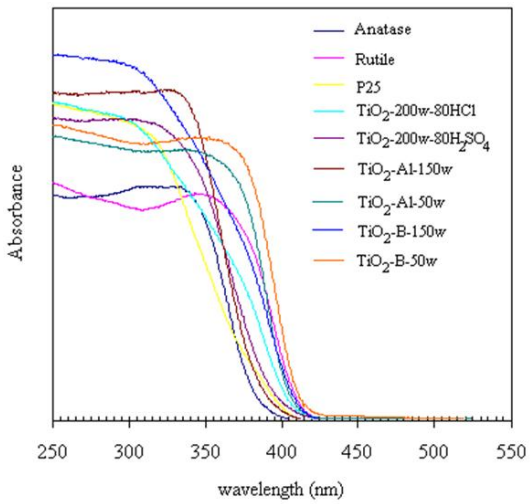

Figure 4. The diffused reflectance spectra of the commercial and the synthesized TiO_2 samples

Table 2. Absorption edge and band gap energy of commercial TiO_2 and synthesized TiO_2 samples.

Sample	Absorption edge (nm)	Bandgap energy [a] (eV)	
		This work	Literature
Anatase	383	3.24	3.20 [b]
Rutile	411	3.02	3.00 [b]
Degussa P25	395	3.14	3.14 [c]
TiO_2-200w-80HCl	406	3.05	-
TiO_2-200w-80H_2SO_4	394	3.15	-
TiO_2-Al-150w	385	3.22	-
TiO_2-Al-50w	405	3.06	-
TiO_2-B-150w	410	3.02	-
TiO_2-B-50w	411	3.02	-

[a] Calculated by Plank's equation: $E_g = 1240/\lambda$.
[b] Sclafani *et al.* (1990); Miao *et al.* (2003).
[c] Zielinska *et al.* (2003)

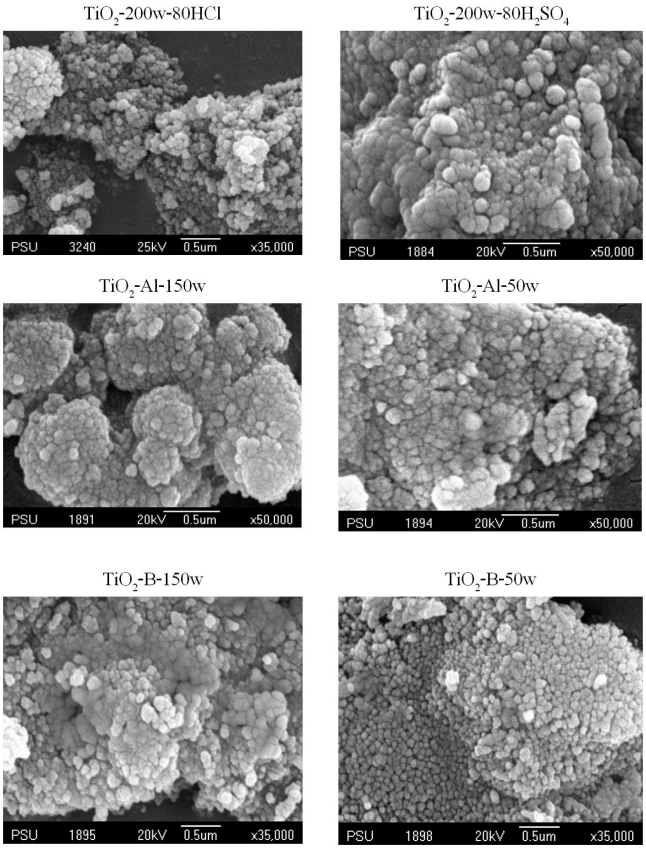

Figure 5. The morphology of synthesized TiO_2 samples.

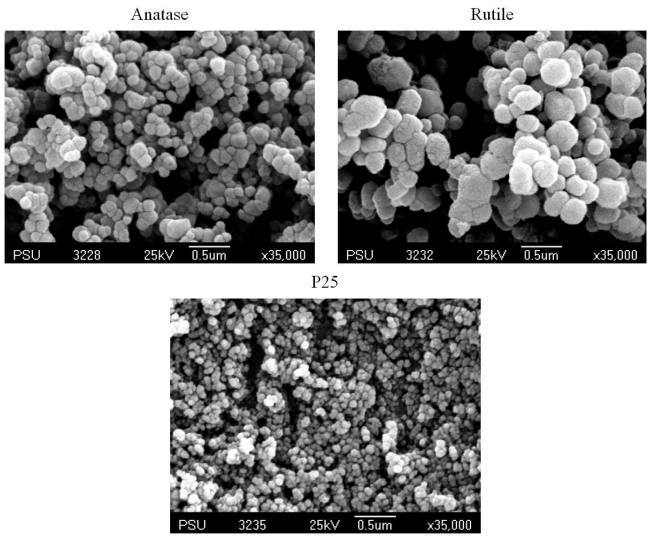

Figure 6. The morphology of commercial TiO_2 samples.

membrane. Under certain conditions, the Gram-negative bacteria are more resistant to many chemical agents than the Gram-positive cells (Tortora *et al.*, 2001).

As shown in Table 3, two of the synthesized samples, TiO_2-200w-80H_2SO_4 and TiO_2-Al-150w, showed the best results in inhibiting the cell growth of all tested bacteria with the lowest amount of titania and irradiation time. Another sample, TiO_2-B-50w, eventhough slightly inferior to the first two samples, also showed better result than P25. The commercial P25 TiO_2, which has been used in many reports with good results, also showed good performance in this test by being able to cause inactivation of all five bacteria, but with higher MIC values than the first three samples. The commercial anatase TiO_2, usually showing slightly lower activity than P25 in the dye degradation study, fails to inactivate *S. aureus* and MRSA bacteria in this test. The commercial rutile did not show any activity at all for all the five bacteria, which is consistent with its poor performance found in the dye degradation study (Kanna and Wongnawa, 2008). Another two of the synthesized samples, TiO_2-A1-50w, TiO_2-B-150w,

Table 3. MIC values of TiO_2 samples with various bacteria.

TiO_2 samples	Irradiation time (min)	MIC (mg/mL)				
		P.aeruginosa	*E.coli*	*B.subtilis*	*S.aureus*	MRSA
Anatase	30	-	-	-	-	-
	60	12.5	-	-	-	-
	90	12.5	100	-	-	-
	120	12.5	12.5	100	-	-
Rutile	30	-	-	-	-	-
	60	-	-	-	-	-
	90	-	-	-	-	-
	120	-	-	-	-	-
Degussa P25	30	-	-	100	-	-
	60	100	100	50	100	100
	90	100	100	25	100	100
	120	100	100	25	100	100
TiO_2-200w-80HCl	30	-	-	-	-	-
	60	-	-	-	-	-
	90	-	-	-	-	-
	120	100	100	100	100	100
TiO_2-200w-80H_2SO_4	30	25	50	25	25	25
	60	25	25	25	25	25
	90	25	25	25	25	25
	120	25	25	25	25	25
TiO_2-Al-150w	30	50	100	50	50	50
	60	25	50	50	50	50
	90	25	50	25	25	25
	120	25	25	25	25	25
TiO_2-Al-50w	30	100	-	-	-	-
	60	100	100	100	-	-
	90	100	100	100	-	-
	120	50	50	50	100	100
TiO_2-B-150w	30	100	-	-	-	-
	60	100	100	100	-	-
	90	100	100	100	-	-
	120	50	50	50	100	100
TiO_2-B-50w	30	100	-	12.5	25	100
	60	100	-	12.5	25	50
	90	50	-	12.5	25	50
	120	50	100	12.5	25	50

* (-) represent the bacterial growth equal to the control (no inhibition)

showed respectable results with all five bacteria. The last one, TiO_2-200w-80HCl, eventhough it could inactivate all five bacteria, it needed a long irradiation time with high MIC values compared with all the synthesized samples in this study. In summary, it is interesting to see that all of the six synthesized samples could inactivate all five bacteria in this screening test albeit with varying MIC values. In comparison with P25, three samples showed better antibacterial activity than P25. The order of performance can be arranged as follows:

TiO_2-200w-80H_2SO_4 > TiO_2-Al-150w > TiO_2-B-50w > P25 > TiO_2-Al-50w ≈ TiO_2-B-150w > TiO_2-200w-80HCl > anatase > rutile.

With regard to the photocatalytic activity, there have been

many reports that the anatase shows higher activivty than the rutile in many photocatalytic reactions in air and water (Mills and Sawunyama, 1994; Sclafani and Herrmann, 1996; Lucarelli *et al.*, 2000; Sato and Taya, 2006) except in some cases (Ohno *et al.*, 1997). The effect of crystalline structures on biocidal activity of TiO_2 particles has been clarified by investigating the photocatalytic deactivation of phage MS2 in suspensions of anatase TiO_2 and rutile TiO_2 as well as their mixtures. The results showed that the contact between both types of TiO_2 particles in aggregations caused the enhancement of the quantum yield of the TiO_2 suspension, thereby the generation of reactive oxygen species from photocatalytic reaction, which leads to the enhancement of biocidal activity of the photocatalytic particles (Sato and Taya, 2006). In another study, the photocatalytic process of anatase has been shown to produce highly reactive species, such as hydroxyl radical, hydrogen peroxide, and superoxide, which, in principle, can cause fatal damage to microorganisms by injury of the cell membranes when bacteria come into contact with the TiO_2 surface (Sunada *et al.*, 1998).

Most of the recent research on the inhibition of bacterial cell growth (Gumy *et al.*, 2006a; Gumy *et al.*, 2006b; Verran *et al.*, 2007) have been studied by using the suspended-TiO_2 in solution. In suspension, TiO_2 nanoparticles were trapped onto the bacteria surface resulting in the adsorption of TiO_2 particles on the bacteria surface, which could lead to the inactivation of bacteria in couple with the photocatalytic oxidation reaction described above. In this study, the agar dilution method was chosen to eliminate the possibility of inactivation by surface adsorption, hence the inactivation results could be said to come solely from the photocatalytic property of the photocatalysts. In this method, the TiO_2 nanoparticles were fixed in agar and would not be adsorbed onto the bacterial surface. The disadvantage of this method is that, due to the fixed TiO_2 particles in the agar matrix, a higher concentration of the photocatalyst is required, and, hence, the MIC values from this method would be higher than that from the suspension method.

Our results as mentioned above showed that the antibacterial activity of the synthesized anatase-type TiO_2, TiO_2-200w-80H_2SO_4 and TiO_2-Al-150w, are more effective than the commercial P25. It is rather difficult to rationalize this surprising behavior. When discussing the photocatalytic activity, the parameters such as bandgap energy, surface area, crystallinity, and phases are usually of prime concerns. The bandgap energy, however, does not seem to be a major factor in this case since the bandgap of TiO_2-B-50w, the third best performer, is only 3.02 eV, which is low compared to the top two performers, TiO_2-200w-80H_2SO_4 and TiO_2-Al-150w, with 3.15 and 3.22 eV, respectively. A pure single anatase phase is active while a pure rutile phase does not show any activity, whereas in the TiO_2-B-50w case it is a mixture of amorphous and rutile phase. Although the clear explanation for the high activity of P25 is still unknown, there seems to have a belief that it is the result of a synergetic effect between the mixed phases of anatase and rutile plus the high crystallinity (Ohno *et al.*, 2001; Ohno *et al.*, 2003). The generally good performance shown by all the six synthesized samples in this work can be narrowed down to their uncalcined nature during the syntheses. Without the calcination, (1) the products are mainly amorphous with a small amount of anatase and/or rutile mixed in, (2) the products have low crystallinity and small crystallite sizes, hence large surface areas. The small crystallite sizes may help disperse the particles within the agar matrix better than the larger ones, ensuring an evenly high concentration of photocatalysts within the agar matrix as well as the agar surface resulting in good inactivation activities. When irradiated with UV light, the reactive oxygen species are generated from the TiO_2 centers at the agar surface and come into contact with bacteria, and by this operate in concert to attack the polyunsaturated phospholipids in the bacteria. The lipid peroxidation reaction causes a breakdown function is the mechanism underlying cell death. The attack by reactive species generated by the photocatalytic process outside the cell is very likely the initial mode of killing that is observed for bacteria and other cell types (Maness *et al.*, 1999).

4. Conclusions

In this study, photocatalyst TiO_2 powders in anatase or rutile or a mixture of anatase and rutile phases have been synthesized from an aqueous solution of $TiCl_4$ by sol-gel process. No calcination at high temperature was applied to these syntheses. The product TiO_2 composed of mainly amorphous phase with a small amount of anatase or rutile or a mixture of both. These samples were tested for antibacterial activity in comparison with the commercial products, anatase, rutile, and Degussa P25. All the six synthesized samples showed inactivation activity towards bacteria, two of them showed a higher activity than Degussa P25.

Acknowledgements

This work was supported by the Songklanagarind Scholarship for Graduate Studies from the Prince of Songkla University.

References

Approved standard M7-A4. 2002. Reference methods for dilution antimicrobial susceptibility tests for bacteria that grow aerobically, Clinical and Laboratory Standards Institute (CLSI), Wayne, PA, USA.

Benabbou, A.K., Derriche, Z., Felix, C., Lejeune, P., and Guillard, C. 2007. Photocatalytic inactivation of *Escherischia coli*: effect of concentration of TiO_2 and microorganism, nature, and intensity of UV irradiation. Applied Catalysis B: Environmental. 76, 257-263.

Cho, M., Chung, H., Choi, W., and Yoon, J. 2004. Linear correlation between inactivation of *E.coli* and OH radical concentration in TiO_2 photocatalytic disinfec-

tion. Water Research. 38, 1069-1077.

Dadjour, M.F., Ogino, C., Matsumura, S., Nakamura, S., and Shimizu, N. 2006. Disinfection of *Legionella pneumophila* by ultrasonic treatment with TiO_2. Water Research. 40, 1137-1142.

Fernández, P., Blanco, J., Sichel, C., and Malato, S. 2005. Water disinfection by solar photocatalysis using compound parabolic collectors. Catalysis Today. 101, 345-352.

Gopal, M., Chan, W.J.M., and Jonghe, L.C.D. 1997. Room temperature synthesis of crystalline metal oxides. Journal of Materials Science. 32, 6001-6008.

Gumy, D., Morais, C., Bowen, P., Pulgarin, C., Giraldo, S., Hajdu, R., and Kiwi, J. 2006a. Catalytic activity of commercial of TiO_2 powders for the abatement of the bacteria (*E. coli*) under solar simulated light: influence of the isoelectric point. Applied Catalysis B: Environmental. 63, 76-84.

Gumy, D., Rincon, A.G., Hajdu, R., and Pulgarin, C. 2006b. Solar photocatalysis for detoxification and disinfection of water: different types of suspended and fixed TiO_2 catalysts study. Solar Energy. 80, 1376-1381.

Hoffmann, M.R., Martin, S.T., Choi, W., and Bahnemann, D.W. 1995. Environmental applications of semiconductor photocatalysis. Chemical Reviews. 95, 69-96.

Huang, Z., Maness, P.C., Blake, D.M., Wolfrum, E.J., Smolinski, S.L., and Jacoby, W.A. 2000. Bactericidal mode of titanium dioxide photocatalysts. Journal of Photochemistry and Photobiology A: Chemistry. 130, 163-170.

Ibanez, J.A., Litter, M. I., and Pizarro, R.A. 2003. Photocatalytic bactericidal effect of TiO_{2-} on *Enterobacter cloacae*: comparative study with other Gram (-) bacteria. Journal of Photochemistry and Photobiology A: Chemistry. 157, 81-85.

Ireland J.C., Klostermann P., Rice E.W., and Clark R.M. 1993. Inactivation of *Escherichia coli* by titanium dioxide photocatalytic oxidation. Applied and Environment Microbiology. 59, 1668-1670.

Jacoby, W.A., Maness, P.C., Wolfrum, E.J., Blake, D.M., and Fennell, J.A. 1998. Mineralization of bacterial cell mass on a photocatalytic surface in air. Environmental Science and Technology. 32, 2650-2653.

Kanna, M. and Wongnawa, S. 2008. Mixed amorphous and nanocrystalline TiO_2 powders prepared by sol-gel method: characterization and photocatalytic study. Materials Chemistry and Physics. 110, 166-175.

Legrini, O., Oliveros, E., and Braun, A.M. 1993. Photochemical processes for water treatment. Chemical Reviews. 93, 671-679.

Lin, C.Y. and Li, C.S. 2003. Inactivation of microorganisms on the photocatalytic surfaces in air. Aerosol Science and Technology. 37, 939-946.

Lonnen, J., Kilvington, S., Kehoe, S.C., Al-Touati, F., and McGuigan, K.G. 2005. Solar and photocatalytic disinfection of protozoan, fungal and bacterial microbes in drinking water. Water Research. 39, 877-883.

Lucarelli, L., Nadtochenko, V., and Kiwi, J. 2000. Environmental photochemistry: quantitative adsorption and FTIR studies during the TiO_2-photocatalyzed degradation of Orange II. Langmuir. 16, 1102-1108.

Maness, P.C., Smolinski, S., Blake, D.M., Huang, Z., Wulfrum, E.J., and Jacoby, W.A. 1999. Bactericidal activity of photocatalytic TiO_2: toward an understanding of its killing mechanism. Applied and Environment Microbiology. 65, 4094-4098.

Matsunaga, T., Tomoda, R., Nakajima, T., and Wake, H. 1985. Photoelectrochemical sterilization of microbial cells by semiconductor powders. Federation of European Microbiological Societies Microbiology Letters. 29, 211-214.

Miao, L., Jin, P., Kaneko, K., Terai, A., Nabatova-Gabain, N., and Tanemura, S. 2003. Preparation and characterization of polycrystalline anatase and rutile TiO_2 thin films by rf magnetron sputtering. Applied Surface Science. 212/213, 255-263.

Mills, A. and Sawunyama, P. 1994. Photocatalytic degradation of 4-chlorophenol mediated by TiO_2: a comparative study of the activity of laboratory made and commercial TiO_2 samples. Journal of Photochemistry and Photobiology A: Chemistry. 84, 305-309.

Mills, A. and Hunte, L.S. 1997. An overview of semiconductor photocatalysis. Journal of Photochemistry and Photobiology A: Chemistry. 108, 1-35.

Ohno, T., Haga, D., Fujihara, K., Kaizaki, K., and Matsumura, M. 1997. Unique effects of Iron(III) ions on photocatalytic and photoelectrochemical properties of titanium dioxide. Journal of Physical Chemistry B. 101, 6415-6419.

Ohno, T., Sarukawa, K., Tokieda, K., and Matsumura, M. 2001. Morphology of a TiO_2 photocatalyst (Degussa, P-25) consisting of anatase and rutile crystalline phases. Journal of Catalysis. 203, 82-86.

Ohno, T., Tokieda, K., Higashida, S., and Matsumura, M. 2003. Synergism between rutile and anatase TiO_2 particles in photocatalytic oxidation of naphthalene. Applied Catalysis A: General. 244, 383-391.

Otaki M., Hirada T., and Ohgaki S. 2000. Aqueous microorganisms inactivation by photocatalytic reaction. Water Science and Technology. 42, 103-108.

Pal, A., Pehkonen, S.O., Yu, L.E., and Ray, M.B. 2007. Photocatalytic inactivation of Gram-positive and Gram-negative bacteria using fluorescent light. Journal of Photochemistry and Photobiology A: Chemistry. 186, 335-341.

Randorn, C., Wongnawa, S., and Boonsin, P. 2004. Bleaching of methylene blue by hydrated titanium dioxide. Science Asia. 30, 149-156.

Rincón, A.G. and Pulgarin, C. 2003. Phtocatalytic inactivation of *E. coli*: effect of (continuous-intermittent) light

intensity and of (suspended-fixed) TiO_2 concentration. Applied Catalysis B: Environmental. 44, 263-284.

Rincón, A.G. and Pulgarin, C. 2004. Effect of pH, inorganic ions, organic matter and H_2O_2 on *E. coli* K12 photocatalytic inactivation by TiO_2: implications in solar water disinfection. Applied Catalysis B: Environmental. 51, 283-302.

Rincón, A.G. and Pulgarin, C. 2006. Comparative evaluation of Fe^{3+} and TiO_2 photoassisted process in solar photocatalytic disinfection of water. Applied Catalysis B: Environmental. 63, 222-231.

Sato, T. and Taya, M. 2006. Enhancement of phage inactivation using photocatalytic titanium dioxide particle with different crystalline structures. Biochemical Engineering Journal. 28, 303-308.

Sclafani, A., Palmisano, L., and Schiavello, M. 1990. Influence of the preparation methods of titanium dioxide on the photocatalytic degradation of phenol in aqueous dispersion. Journal of Physical Chemistry. 94, 829-832.

Sclafani, A. and Herrmann, J.M. 1996. Comparison of the photoelectronic and photocatalytic activities of various anatase and rutile forms of titania in pure liquid organic phase and in aqueous solutions. Journal of Physical Chemistry. 100, 13655-13661.

Sichel, C., de Cara, M., Tello, J., Blanco, J., and Fernández-Ibáñez, P. 2007. Solar photocatalytic disinfection of agricultural pathogenic fungi: *Fusarium* species. Applied Catalysis B: Environmental. 74, 152-160.

Sivalingam, G., Nagaveni, K., Hegde, M.S., and Madras, G. 2003. Photocatalytic degradation of various dyes by combustion synthesized nano anatase TiO_2. Applied Catalysis B: Environmental. 45, 23-38.

Sökmen, M., Deðgerli, S., and Aslan, A. 2008. Photocatalyitc disinfection of *Giardia intestinalis* and *Acanthamoeba castellani cysts* in water. Experimental Parasitology. 119, 44-48.

Stylidi, M., Kondarides, D.I., and Verykios, X.E. 2004. Visible light-induced photocatalytic degradation of acid orange 7 in aqueous TiO_2 suspensions. Applied Catalysis B: Environmental. 47, 189-201.

Sunada, K., Kikuchi, Y., Hashimoto, K., and Fujishima, A. 1998. Bactericidal and detoxification effects of TiO_2 thin film photocatalysts. Environmental Science and Technology. 32, 726-728.

Suwanchawalit, C. 2005. The effect of metal-doping on the physical and photocatalytic properties of nanosized TiO_2 powder, M.S. Thesis, Prince of Songkla University, Thailand.

Tortora, G., Funke, R.B., and Case, L.C. 2001. Microbiology: An Introduction, Addison-Wesley Longman, Inc., New York, USA.

Verran, J., Sandoval, G., Allen, N.S., Edge, M., and Stratton, J. 2007. Variables affecting the antibacterial properties of nano and pigmentary titania particles in suspension. Dyes and Pigments. 73, 298-304.

Yao, K.S., Wang, D.Y., Ho, W.Y., Yan, J.J., and Tzeng, K.C. 2007. Photocatalytic bactericidal effect of TiO_2 thin film on plant pathogens. Surface and Coatings Technology. 201, 6886-6888.

Zhang, Q.H., Guo, J.K., and Gao, L. 1999. Preparation and characterization of nanosized TiO_2 powders from aqueous $TiCl_4$ solution. Nanostructured Materials. 11, 1293-1300.

Zhang, Q., Gua, J., and Gao, L. 2000. Effect of hydrolysis conditions on morphology and crystallization of nanosized TiO_2 powder. Journal of European Ceramic Society. 20, 2153-2158.

Zieliñska, B., Grzechulska, J., Grzmil, B., and Morawski, A.W. 2001. Photocatalytic degradation of Reactive Black 5: a comparison between TiO_2-Tytanopol A11 and TiO_2 Degussa P25 photocatalysts. Applied Catalysis B: Environmental. 35, L1-L7.

Zieliñska, B., Grzechulska, J., Kaleñczuk, R.J., and Morawski, A.W. 2003. The pH influence on photocatalytic decomposition of organic dyes over A11 and P25 titanium dioxide. Applied Catalysis B: Environmental. 45, 293-300.